Journal of Thermophysics and Heat Transfer
Vol. 22, No. 3, July–September 2008

Thermal Effectiveness Correlation for a Shell and Tube Condenser with Noncondensing Gas

Y. Haseli,* I. Dincer,† and G. F. Naterer‡
University of Ontario Institute of Technology, Oshawa, Ontario L1H 7K4, Canada

DOI: 10.2514/1.34735

This paper analyzes the local effectiveness of a baffled horizontal shell and one-path tube condenser along the condensation path, including leakage of air as a noncondensing gas. Condensation of steam occurs in the shell side, and cooling water flows through the tubes. A new formulation is developed for the maximum heat transfer rate between two streams in the heat exchanger, when one stream undergoes a condensation process. The effects of air mass flow rate, upstream cooling water, steam-air mixture temperatures, steam flow rate, and cooling water flow rate on the effectiveness along the exchanger are numerically investigated. The results lead to a new correlation for the thermal effectiveness as a function of upstream cooling water temperature, air mass flow rate, heat capacitance ratio, and dimensionless temperature, defined as the ratio of the cooling water temperature gradient to the difference between the condensation and inlet cooling water temperatures. Furthermore, an analytical expression is derived for the exergy efficiency of the system, which shows how irreversibilites characterized by the entropy generation number and environment temperature affect the second law efficiency. Typical results of this expression are compared with results from past numerical work. Close agreement between these comparisons provide useful validation of the current model.

Nomenclature

A	=	heat transfer area, m^2
C	=	heat capacitance, kJ/K
c	=	heat capacitance ratio, C_{cond}/C
c_p	=	specific heat, kJ/kg K
e	=	specific flow exergy, kJ/kg
g	=	steam-air mixture
h	=	enthalpy, kJ/kg
h_{fg}	=	condensation latent heat, kJ/kg
k_1, k_2	=	coefficients in Eq. (16)
$\dot{m}$	=	mass flow rate, kg/s
N_s	=	entropy generation number, Eq. (26)
$\dot{Q}$	=	heat transfer rate, kW
$\dot{S}$	=	entropy generation rate, kJ/s K
s	=	entropy, kJ/kg K
T	=	temperature, °C
T_o	=	dead state/environment temperature, °C
U	=	overall heat transfer coefficient, kW/m^2 K
ε	=	effectiveness
η_{ex}	=	exergy efficiency
θ	=	dimensionless temperature, Eq. (11)

Subscripts

a	=	air
c	=	coolant
cond	=	condensate
cw	=	cooling water
in	=	inlet
max	=	maximum
out	=	outlet
s	=	steam
v	=	vapor

I. Introduction

CONDENSATION heat transfer and its application in industry have been widely studied, both experimentally and theoretically, by many researchers. A horizontal shell and tube condenser, in which condensation takes place outside of single tubes, is one of the most common configurations that is used for industrial purposes, such as power and process industries. Browne and Bansal [1] have reviewed past advances in condensation heat transfer in this type of condenser for different geometries of tubes. Useful correlations for design and modeling purposes have been included in their study, such as correlations that consider the effects of tube banks and vapor shear on the condensation heat transfer coefficient.

Past studies have focused on the enhancement of condensation heat transfer, thereby increasing the thermal effectiveness of a heat exchanger. For instance, Semenov et al. [2] analyzed the behavior of the coefficients of heat transfer on noncircular horizontal pipes, whose cross sections have profiles with curvature continuously decreasing from the upper to lower generatrix. They showed that the coefficient of heat transfer during condensation of steam on such tubes is 20–30% greater than on circular pipes. Xie and Eckels [3] performed experiments to measure the shell side heat transfer coefficient of condensation of HFC-134a on the following three types of horizontal test tubes: enhanced, two-dimensional finned, and three-dimensional enhanced. They reported that the enhanced tubes significantly improved the condensation heat transfer effectiveness compared with the smooth tube, with the 3-D enhanced tube having the highest heat transfer coefficients.

Briggs [4] has recently presented an overview of the use of low-fin or minifin tubes for improving the heat transfer performance in shell side condensers. The experimental and theoretical work was performed at the Queen Mary University of London. It has resulted in an extensive database of experimental data for condensation on single tubes, covering a wide range of tube geometries and fluid thermophysical properties. It led to the development of a useful model that predicts the majority of this data to within 20%. This work progresses on those past studies to examine the effects of vapor shear

Received 23 September 2007; revision received 27 December 2007; accepted for publication 20 January 2008.

*M.S. Candidate, Faculty of Engineering and Applied Science, 2000 Simcoe Street North; yousef.haseli@mycampus.uoit.ca.

†Professor of Mechanical Engineering, Faculty of Engineering and Applied Science, 2000 Simcoe Street North; ibrahim.dincer@uoit.ca.

‡Professor and Director of Research, Graduate Studies and Development, Faculty of Engineering and Applied Science, 2000 Simcoe Street North; greg.naterer@uoit.ca.

and three-dimensional fin profiles; the latter has shown potential for higher heat transfer enhancement.

The thermal effectiveness, ε, of a heat exchanger is the ratio of the heat transfer rate to the maximum possible heat transfer rate. The relevant explicit equations relating the effectiveness to the number of transfer units (NTU) and the configuration of a heat exchanger are available in heat transfer references, that is, Lienhard and Lienhard [5] and Incropera [6]. Past literature shows studies that have used the ε–NTU method when studying the condenser type of exchangers. An example is past work of Berg and Berg [7]. They developed an analytic method to describe the flow in each row of tubes of an air-cooled, one-pass, isothermal condenser. They used the NTU approach to derive expressions for the pressure drop in each row, in terms of the exchanger effectiveness. The resulting simultaneous equations were solved numerically. The solutions were presented graphically, showing the flow pattern to be solely a function of effectiveness. Another example is the past work of Kayansayan [8], who described an effectiveness-NTU method for bayonet-tube evaporators and condensers. The fluid temperature distribution and exchanger effectiveness were presented as a function of the Hurd number, NTU, and flow arrangement. The numerical method of Kayansayan was applicable only for evaporators and condensers with pure fluids. More recently, Wright and Heggs [9] developed a methodology to predict the effectiveness of a single pass, two stream plate heat exchanger when one stream undergoes a phase change (specifically condensation). Analytical solutions were given for the system under the assumption of a constant overall heat transfer coefficient, when operated in either cocurrent or countercurrent arrangements. The analysis was then extended to systems in which the overall heat transfer correlation is dependent on the quality of the phase-change stream.

Based on the general definition of the thermal effectiveness of heat exchangers, a modification is first presented in this paper to evaluate the effectiveness of a condenser when a pure vapor undergoes phase change. Then, it is extended to the analysis of local effectiveness of condensation of steam from a mixture of air in a TEMA "E" shell and tube exchanger. Based on the numerical findings, a correlation is developed to assess the effectiveness for a certain operating condition and arbitrary position along the condenser. Moreover, an explicit equation is presented in the last part of this paper to show how thermal irreversibilities are related to the exergy efficiency of the system.

II. Formulation of Thermal Effectiveness of a Condenser

The thermal effectiveness of a heat exchanger is described as the ratio of the real heat transfer rate to the maximum possible heat transfer rate within the exchanger:

$$\varepsilon = \frac{\dot{Q}}{\dot{Q}_{\max}} \tag{1}$$

The maximum heat transfer between two certain streams in a heat exchanger may occur when the stream of the lower heat capacity experiences the maximum temperature difference, defined as the difference between inlet temperatures of hot and cold fluids. For the specific and known inlet temperatures and mass flow rates of both fluids, the maximum heat transfer may theoretically occur if the effective heat transfer area is infinite. This implies that the surface area is the only constraint for theoretically achieving the maximum heat transfer rate. However, this does not hold for the case of a phase-change process within the heat exchanger, which will be specifically considered below.

Based on the conventional definition of the maximum heat transfer rate in heat exchangers, as mentioned in past heat transfer references, when a heat exchanger undergoes a phase-change process like condensation, the maximum heat transfer rate occurs if the coolant experiences a temperature rise equal to the difference between its inlet and the condensation temperatures, that is, $\dot{Q}_{\max}= C_c(T_{\mathrm{cond}} - T_{c,\mathrm{in}})$. It should be noted that this equality to represent the maximum heat transfer rate is not only subject to the heat transfer area. Assuming that the heat exchanger has a sufficient heat transfer area to condense the vapor, in contrast to ordinary heat exchange without phase change, increasing the effective surface area and the mass flow rate of vapor are required for a continuous rise of coolant temperature gradient to reach the condensation temperature. Therefore, the maximum heat transfer rate is subject to two factors, unlike the conventional definition of the maximum heat transfer rate between two fluid streams in heat exchangers discussed in the preceding paragraph. Establishing the aforementioned maximum heat transfer rate is not defined for two specific streams, as the flow rate of hot fluid needs to be increased. However, this leads to an alternative definition of the maximum heat transfer rate between two specific streams in a condenser as follows. The maximum possible heat transfer rate between the condensing fluid and coolant stream would occur if these two streams were brought to thermal equilibrium. In other words, after condensing all vapor, whichever among the condensate and coolant is the first to experience its maximum possible temperature difference, that stream would lead to the maximum heat transfer rate. It can be now expressed in mathematical terms as

$$\dot{Q}_{\max} = \dot{Q} + \min\begin{Bmatrix} C_{\mathrm{cond}}(T_{\mathrm{cond}} - T_{c,\mathrm{in}}) \\ C_c(T_{\mathrm{cond}} - T_{c,\mathrm{out}}) \end{Bmatrix} \tag{2}$$

where

$$\dot{Q} = \dot{m}_v h_{fg} = C_c(T_{c,\mathrm{out}} - T_{c,\mathrm{in}}) \tag{3}$$

Equation (2) supplemented with Eq. (3) implies that thermal equilibrium between two streams in a condenser might occur after condensation of the vapor, if either the condensate first reaches its maximum temperature difference, that is, $T_{\mathrm{cond}} - T_{c,\mathrm{in}}$, or the coolant experiences a maximum temperature difference of $T_{\mathrm{cond}} - T_{c,\mathrm{out}}$. The following subsections investigate individually these two cases.

A. Case 1: $C_{\mathrm{cond}}(T_{\mathrm{cond}} - T_{c,\mathrm{in}}) > C_c(T_{\mathrm{cond}} - T_{c,\mathrm{out}})$

Combining Eqs. (2) and (3), the maximum heat transfer rate is

$$\dot{Q}_{\max} = C_c(T_{\mathrm{cond}} - T_{c,\mathrm{in}}) \tag{4}$$

Substituting Eqs. (3) and (4) into Eq. (1) gives

$$\varepsilon = \frac{T_{c,\mathrm{out}} - T_{c,\mathrm{in}}}{T_{\mathrm{cond}} - T_{c,\mathrm{in}}} \tag{5}$$

The differential energy equation representing augmentation of the coolant side energy due to condensation of vapor may be derived as

$$\dot{m}_c c_{p,c}\, \mathrm{d}T_c = U(T_{\mathrm{cond}} - T_c)\, \mathrm{d}A \tag{6}$$

Integrating Eq. (6) from the inlet to the outlet of the condenser yields

$$\frac{T_{\mathrm{cond}} - T_{c,\mathrm{out}}}{T_{\mathrm{cond}} - T_{c,\mathrm{in}}} = \exp\left(-\frac{UA}{C_c}\right) \tag{7}$$

Combining Eqs. (5) and (7) results in

$$\varepsilon = 1 - \exp\left(-\frac{UA}{C_c}\right) \tag{8}$$

which is usually used to assess the effectiveness of condenser type of exchangers. Equation (8) may only be used in thermal analysis of a condenser when $(C\Delta T)_{\mathrm{condensate}} > (C\Delta T)_{\mathrm{coolant}}$, which is often unlikely, as in most applications like the power generation industry, $C_{\mathrm{coolant}} \gg C_{\mathrm{condensate}}$ (due to a larger coolant mass flow rate, compared with condensate). This underlies the key point for which the definition of the maximum heat transfer rate proposed in the current work becomes crucial because, in the second case when $(C\Delta T)_{\mathrm{coolant}} > (C\Delta T)_{\mathrm{condensate}}$, Eq. (8) is no longer valid. However, it has been commonly used in the evaluation of the condenser effectiveness in past literature, thereby leading to incorrect evaluation of the condenser performance. When the heat capacitance of a coolant is much larger than that of the condensate, which practically yields $(C\Delta T)_{\text{coolant}} > (C\Delta T)_{\text{condensate}}$, the resultant expression for the condenser effectiveness is not Eq. (8).

B. Case 2: $C_{\text{cond}}(T_{\text{cond}} - T_{c,\text{in}}) < C_c(T_{\text{cond}} - T_{c,\text{out}})$

The maximum heat transfer rate can be written as

$$Q_{\max} = C_c(T_{c,\text{out}} - T_{c,\text{in}}) + C_{\text{cond}}(T_{\text{cond}} - T_{c,\text{in}}) \tag{9}$$

Thus, the effectiveness of the condenser becomes

$$\varepsilon = \frac{C_c(T_{c,\text{out}} - T_{c,\text{in}})}{C_c(T_{c,\text{out}} - T_{c,\text{in}}) + C_{\text{cond}}(T_{\text{cond}} - T_{c,\text{in}})} \Rightarrow \varepsilon = \frac{1}{1 + c/\theta} \tag{10}$$

where c is the heat capacitance ratio defined as $c = C_{\text{cond}}/C_c$ and

$$\theta = \frac{T_{c,\text{out}} - T_{c,\text{in}}}{T_{\text{cond}} - T_{c,\text{in}}} \tag{11}$$

On the other hand, substituting Eq. (7) into Eq. (10) gives

$$\varepsilon = \frac{1}{1 + \frac{c}{1-\exp(-UA/C_c)}} \tag{12}$$

In addition to the number of transfer units ($\text{NTU} = UA/C_c$) in Eq. (8), another dimensionless parameter appears in Eq. (12), namely "c." Thus, not only is the effectiveness of the condenser influenced by the NTU, but it is also affected by the heat capacitance ratio. A comparison of Eq. (12) at various heat capacitance ratios, c, in the range of 0.01–0.2 with Eq. (8) is illustrated in Fig. 1. From Fig. 1, depending on whether the maximum heat transfer rate is achieved through case 1 or 2, the effectiveness of the condenser may increase or decrease with the NTU, respectively. Each of the graphs based on Eq. (12) has a threshold at approximately $\text{NTU} = 3$. Therefore, values of the NTU greater than 3 do not have a significant influence on the effectiveness.

According to Fig. 1, it can be observed that a higher NTU in a condenser would lead to less effective performance of the heat exchanger. The first predominant parameter lies in the ratio of heat capacitances of the coolant and condensate stream, from which the condenser effectiveness might increase or decrease with the NTU, as the second important factor. This analysis provides a condenser designer with a better understanding of its performance and reveals deeper insight into the process, which could eventually lead to better decisions of operating conditions (involving thermophysical properties of fluids, mass flow rates, heat transfer coefficient, etc.), during the design or performance of condensing heat exchangers.

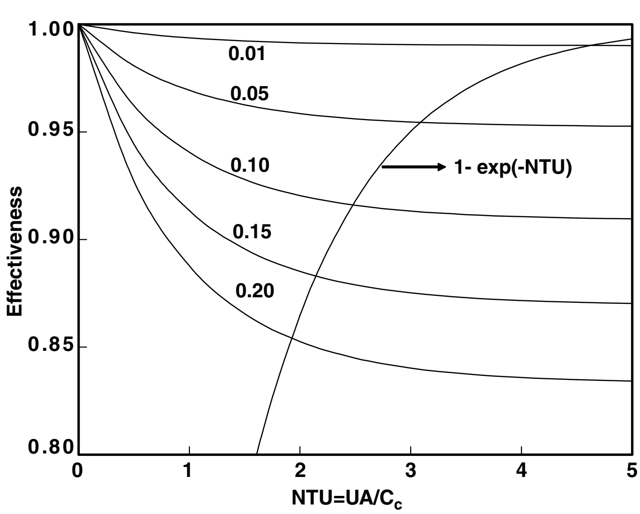

Fig. 1 Comparison of thermal effectiveness of a condenser based on a new definition at different heat capacitance ratios, c, with a conventional equation available in the literature.

III. Effectiveness of a Condenser with Leakage of a Noncondensing Gas

This section focuses on an investigation of the thermal effectiveness along a counterflow TEMA "E" type shell and tube condenser, for which condensation of steam occurs in the shell side, taking into consideration the leakage of air that is common in practical applications. Cooling water is used as the coolant. The condenser is schematically shown in Fig. 2. Inlet and outlet flows at the boundary of an arbitrary control volume of a condenser are presented in Fig. 3. The total heat transfer rate of the cooling water consists of two sources: sensible heat and latent heat (e.g., see Haseli and Roudaki [10]). To determine the effectiveness of the exchanger within the control volume, the maximum heat transfer rate must first be defined. Based on the general definition, the maximum heat transfer rate between two certain streams would take place when they are brought to thermal equilibrium. Thus, for a system of steam-air mixture and cooling water shown in Fig. 3, the maximum heat transfer rate first consists of heat transfer due to condensation of the entire inlet flow rate of steam, $\dot{m}_{s1}$:

$$\dot{Q}_1 = \dot{m}_{s1} h_{fg} \tag{13}$$

As discussed in the previous section, the second term of the maximum heat transfer rate depends on whether the condensate (as well as air in this discussion) or cooling water first experiences the maximum possible temperature difference.

$$\dot{Q}_2 = \min(\dot{Q}'_2, \dot{Q}''_2) \tag{14a}$$

$$\dot{Q}'_2 = (C_{\text{cond}} + C_a)(T_{\text{cond}} - T_{\text{cw},1}) \tag{14b}$$

$$\dot{Q}''_2 = C_{\text{cw}}(T_{\text{cond}} - T'_{\text{cw},2}) \tag{14c}$$

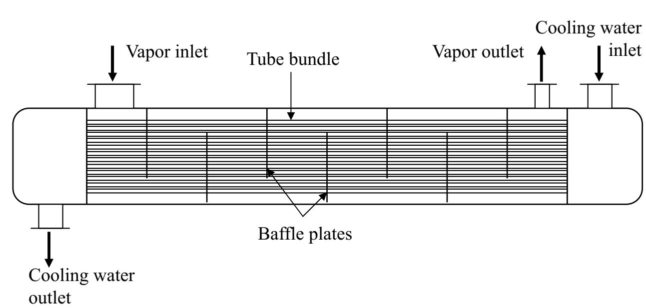

Fig. 2 Countercurrent TEMA "E" shell and tube condenser.

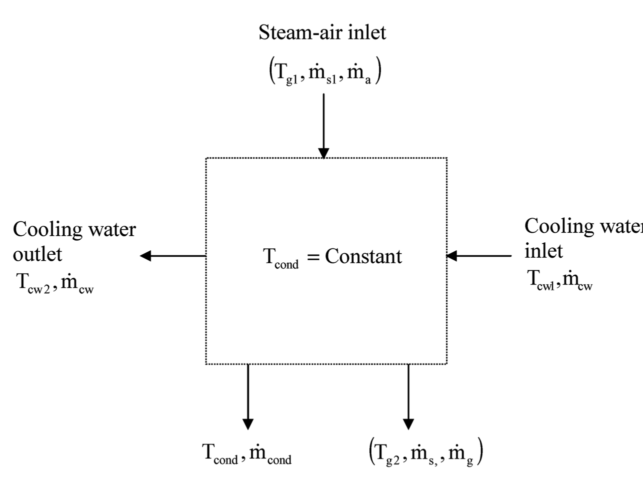

Fig. 3 Control volume of the condenser, illustrating the inlet and outlet flows.

Hence,

$$\dot{Q}_{\max} = \dot{Q}_1 + \dot{Q}_2 \tag{15}$$

Condensation of the entire inlet vapor, $\dot{m}_{s1}$, would require a higher cooling water temperature at the outlet of the control volume represented by $T'_{\mathrm{cw},2}$ in Eq. (14c).

A. Results

The resulting profiles of the effectiveness along a typical industrial condenser studied in previous works [11–13] are presented in this section. The local heat transfer rate within the heat exchanger and maximum possible rate will be determined. This will be carried out with a numerical method developed by Haseli and Roudaki [14] based on a "film model," which solves simultaneously the heat and mass transfer equations along a condensation path and consequently calculates the temperature and condensation rate profiles within a condenser. This method has been recently implemented by Haseli et al. [11] to study entropy production and exergy efficiency of a condenser [12]. In this current work, however, it examines the maximum heat transfer rate through Eqs. (13–15), in addition to the predicted local heat transfer rate, to finally evaluate the local effectiveness. The effects of various process parameters, such as the upstream cooling water temperature, air mass flow rate, upstream steam-air temperature, upstream steam flow rate, and the cooling water mass flow rate, on the effectiveness are investigated. The results are illustrated in Figs. 4–8. As observed in these figures, in general, all effectiveness profiles have increasing trends from the entrance of the steam-air mixture to the last baffle spaces, from which air and noncondensed steam are extracted. At the first baffle space, the difference between thermal energy levels of the shell side and tube side fluids is maximum, whereas only a certain fraction of this energy is transferred from the hot stream to the cold stream. However, as condensation of steam (major source of heat transfer) takes place and the steam-air mixture becomes cooler (as the entrance mixture is superheated) along the condenser, the thermal energy difference between hot and cold streams decreases. This energy difference leads to the maximum heat transfer rate between two streams.

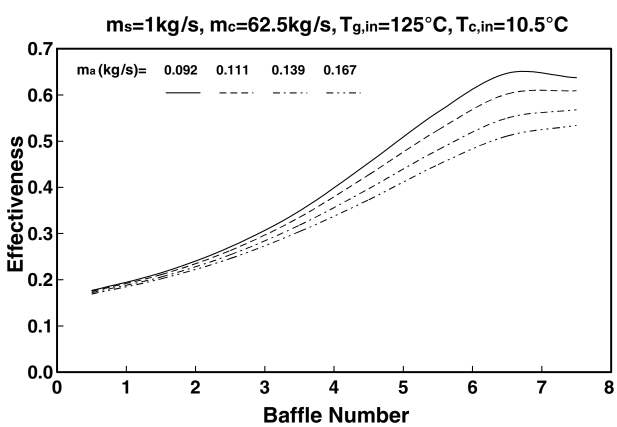

Fig. 4 Effects of air mass flow rate on the effectiveness.

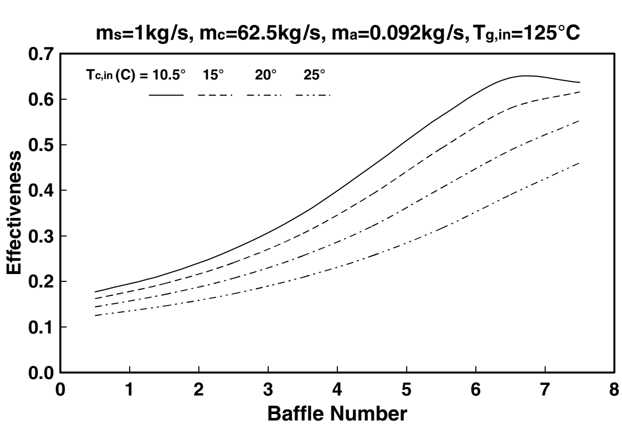

Fig. 5 Effects of the inlet cooling water temperature on the effectiveness.

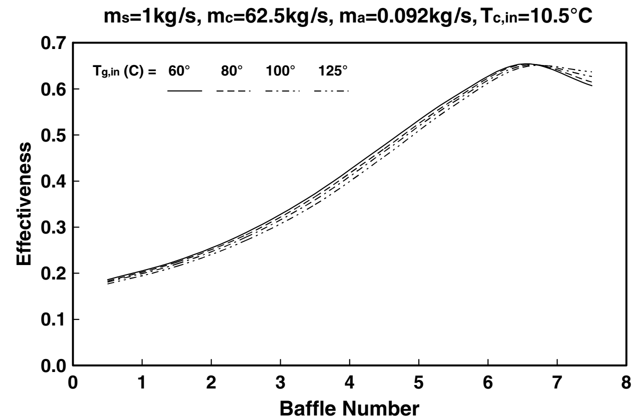

Fig. 6 Effects of the upstream steam-air mixture temperature on the effectiveness.

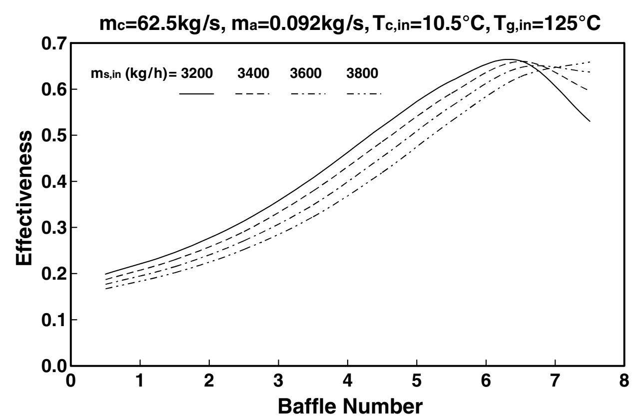

Fig. 7 Effects of the upstream steam mass flow rate on the effectiveness.

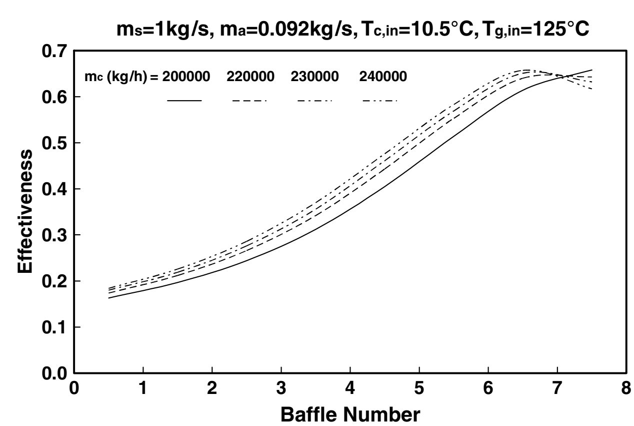

Fig. 8 Effects of the cooling water mass flow rate on the effectiveness.

1. *Effects of the Air Mass Flow Rate*

Figure 4 shows the effect of air leakage on the effectiveness of the exchanger along the condensation path. Near the first baffle spaces, increasing the air leakage leads to only a slight reduction in the effectiveness, whereas as condensation takes place along the exchanger, its influence becomes more significant. Specifically at the last few baffle spaces, a higher air mass flow rate results in a considerable decrease of the effectiveness. In fact, as the air leakage increases, the condensation rate and heat transfer decrease, because of the heat and mass transfer resistance. Because of a higher steam mass fraction at the first few baffle spaces, however, the effect of increasing the air mass flow rate is not significant. As the condensation proceeds, the air fraction quickly becomes dominant at a higher air mass flow rate, which reduces the condensation rate of steam. The effectiveness profile at an air mass flow rate of 0.092 kg/s in Fig. 4 has a peak point. Past studies of Haseli and Roudaki [10] have shown that condensation of steam is almost finalized at this region, under the process condition shown in Fig. 4.

2. Effect of Upstream Cooling Water Temperature

Figure 5 illustrates how increasing the inlet cooling water temperature influences the local effectiveness of the condenser. Increasing the inlet cooling water temperature at the same process condition results in decreasing the condensation and heat transfer rate as the driving temperature force decreases. Further discussion is given by Haseli [15]. A higher water cooling temperature leads to an increase of thermal energy and consequently a decrease in the maximum heat transfer rate between the shell side and cold side. However, decreasing the heat transfer rate by increasing the inlet cooling water temperature is predominant. The profile with a higher inlet cooling water temperature in Fig. 5 is lower.

3. Effects of the Upstream Steam-Air Temperature

The effects of the upstream steam-air mixture temperature in the range of 60–125°C on the effectiveness are depicted in Fig. 6. As expected, a change in steam-air temperature at the same operating condition has only a slight effect on the effectiveness. A higher inlet steam-air mixture results in decreasing the effectiveness. As the main source of heat transfer is the condensation of steam, a higher inlet steam-air temperature causes a slight increase in the maximum heat transfer rate. In other words, as the upstream steam-air mixture is desuperheated, the difference between the energy levels of the mixture and cooling water decreases relatively. This leads to enhancing the effectiveness.

As shown in Fig. 6, all graphs have a maximum point between the sixth and seventh baffle spaces. As outlined previously, the condensation process is almost finished in this region. Also, the profile of the lower upstream temperature reaches its peak point quicker and has a sharper slope after that point. At a higher upstream temperature of the steam-air mixture, the temperature drop of the shell side and, therefore, the sensible heat transfer rate is higher, particularly in the last baffle spaces.

4. Effects of the Upstream Mass Flow Rate of Steam

Figure 7 shows the influence of the upstream mass flow rate of steam on the effectiveness along the condenser. A lower inlet mass flow rate of steam to be condensed contains less energy. Therefore, the maximum heat transfer rate is lower. For the same rate of condensation, the thermal effectiveness is consequently higher. Moreover, at lower upstream mass flow rates of steam, the condensation process finalizes relatively sooner and the role of sensible heat transfer becomes dominant. For this reason, the effectiveness profile of the lower steam flow rate stands lower at the last part of the exchanger. However, from Fig. 7, the corresponding profile of the mass flow rate of 3800 kg/h tends to increase, even in the last baffle space, which shows that condensation of steam occurs in the last baffle space.

5. Effects of the Cooling Water Mass Flow Rate

The cooling water mass flow rate is the last parameter that will be investigated to observe its effect on the local effectiveness. The results for different flow rates of cooling water are depicted in Fig. 8. Decreasing the mass flow rate of cooling water implies that the energy difference between the steam-air mixture stream and the cooling water stream becomes higher. On the other hand, due to conservation of energy in the tube side, a lower mass flow rate of cooling water results in a rise in its temperature gradient. This causes an increase in enthalpy of the cooling water. However, the latter increase is not large compared with the enthalpy of the steam-air mixture. As a result, a lower effectiveness profile may result from lowering the cooling water mass flow rate.

B. Formulation of a Correlation for the Thermal Effectiveness

Another numerical study is performed to investigate a relationship between the effectiveness, ε, and c/θ, from Eq. (10). The effects of process parameters discussed in the previous section on the variation of the effectiveness versus c/θ will be studied. It is observed that the trend of $\varepsilon - c/\theta$ does not respond to a change in any of the following parameters: the upstream steam-air mixture temperature, the upstream mass flow rate of steam, and the cooling water mass flow rate (Fig. 9). Further results involve considerable influence when changing the inlet cooling water temperature or the air mass flow rate on the relationship between the effectiveness and parameter c/θ. The corresponding profiles at different upstream cooling water temperatures and various air leakages are represented in Figs. 10 and 11, respectively. An exponential relationship between ε and c/θ can be observed from the curves in Figs. 10 and 11. We propose the following new correlation that incorporates the local effectiveness, c/θ, the air mass flow rate, and the inlet cooling water temperature as follows:

$$\varepsilon = \exp\left\{-\left[k_1\left(\frac{c}{\theta}\right) + k_2\right]\right\} \qquad \begin{cases} T_{\mathrm{cw,in}} = 10\text{–}30^\circ\mathrm{C} \\ \dot{m}_a = 0.092\text{–}0.250\ \mathrm{kg/s} \end{cases} \tag{16}$$

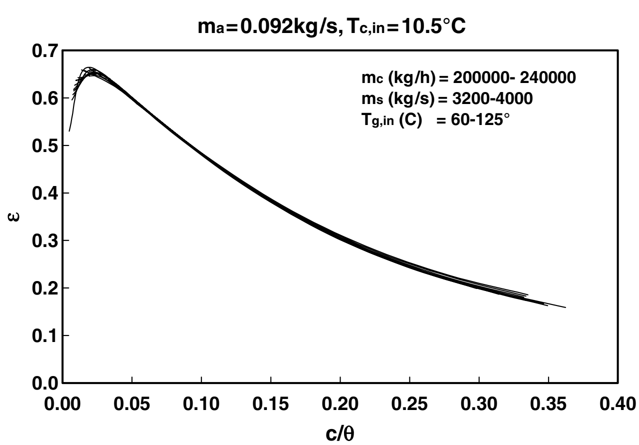

Fig. 9 Dependence of the local effectiveness on c/θ at various cooling water mass flow rates, upstream mass flow rates of steam, and upstream steam-air mixture temperatures.

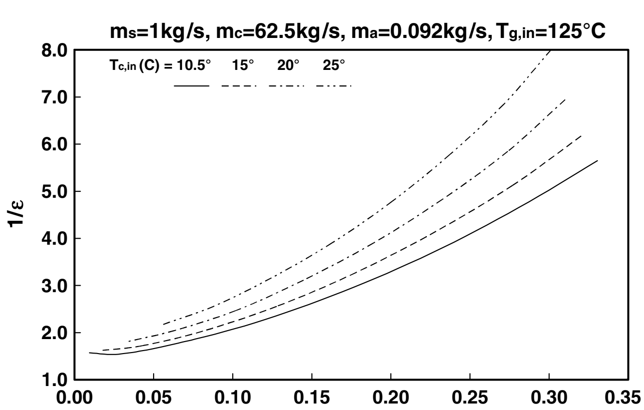

Fig. 10 Effects of the upstream cooling water temperature on the local effectiveness.

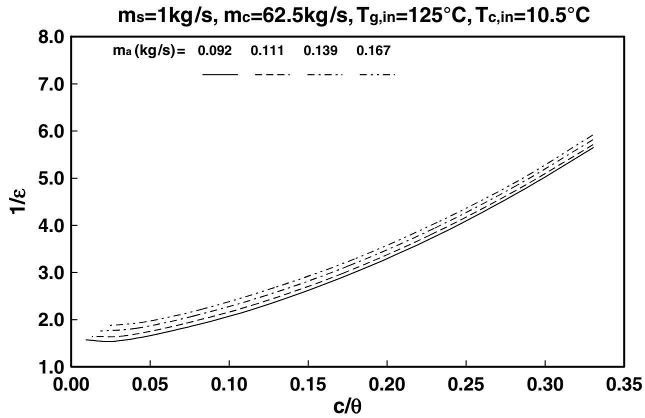

Fig. 11 Effects of the air mass flow rate on the local effectiveness.

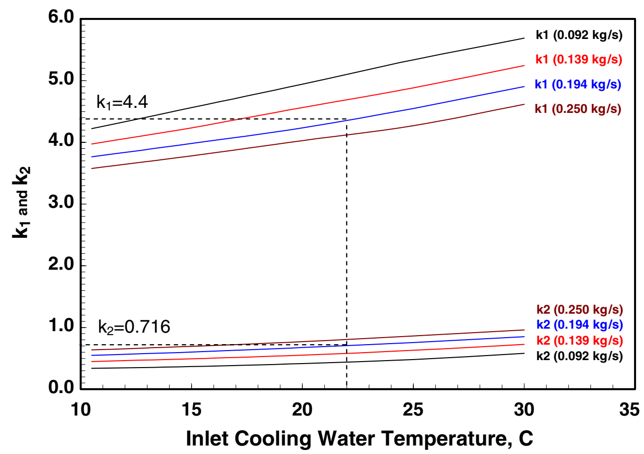

Fig. 12 Dependence of k_1 and k_2 on the inlet cooling water temperature and air leakage (numbers inside the parentheses represent the mass flow rate of air).

where k_1 and k_2 are functions of the inlet cooling water temperature and air mass flow rate. Figure 12 is prepared for this purpose. It shows how one may determine values of k_1 and k_2 at given values of the inlet cooling water temperature and air mass flow rate. As an example, when $T_{\mathrm{cw,in}} = 22°\mathrm{C}$ and $\dot{m}_a = 0.194$ kg/s, $k_1 = 4.4$ and $k_2 = 0.716$ are obtained from Fig. 12. For the values of the air mass flow rates between those shown in Fig. 12, an interpolation method can be used to determine the values of k_1 and k_2 at a known inlet cooling water temperature. Typical representative graphs of $\varepsilon - c/\theta$ are illustrated in Fig. 13. It is observed that at $(c/\theta) > 0.28$, the

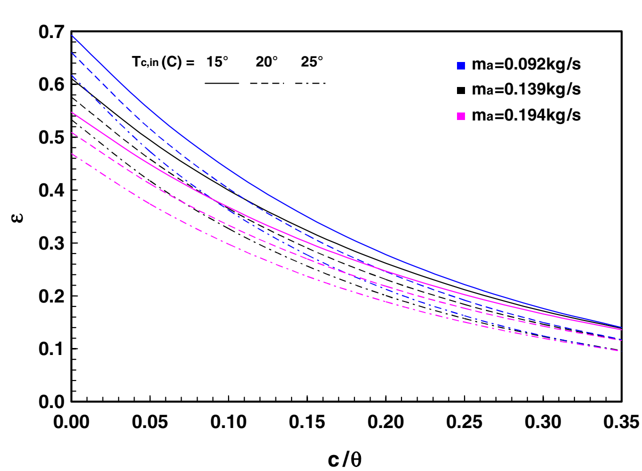

Fig. 13 Variation of the local effectiveness with c/θ at various inlet cooling water temperatures and different air mass flow rates.

effectiveness is approximately independent of the air mass flow rate. This trend is related to the first few baffle spaces in which the mass fraction of steam is much greater than that of air.

IV. Exergy Analysis

Following past work by Haseli et al. [12], in which the exergy efficiency of a condenser was investigated at different process conditions, an explicit expression will be developed herein. This relates the irreversibilities of the process through an entropy generation number to the exergy efficiency. For the control volume shown in Fig. 3, the exergy efficiency may be expressed as [12]

$$\eta_{\mathrm{ex}} = \frac{\dot{m}_{\mathrm{cw}}(e_{\mathrm{cw2}} - e_{\mathrm{cw1}})}{\dot{m}_{s2}(m_{s1} - e_{s2}) + \dot{m}_a(e_{a1} - e_{a2}) + \dot{m}_{\mathrm{cond}}(e_{s1} - e_{\mathrm{cond}})} \tag{17}$$

where e denotes the specific flow exergy. Also, the net change of flow exergy $(e_2 - e_1)$ is evaluated as follows [16]:

$$e_2 - e_1 = h_2 - h_1 - T_o(s_2 - s_1) \tag{18}$$

Hence,

$$\begin{aligned}\dot{m}_{\mathrm{cw}}(e_{\mathrm{cw2}} - e_{\mathrm{cw1}}) &= \dot{m}_{\mathrm{cw}}[h_{\mathrm{cw2}} - h_{\mathrm{cw1}} - T_o(s_{\mathrm{cw2}} - s_{\mathrm{cw1}})] \\ &= Q - T_o\dot{m}_{\mathrm{cw}}(s_{\mathrm{cw2}} - s_{\mathrm{cw1}})\end{aligned} \tag{19}$$

where $\dot{Q}$ is the heat transfer rate absorbed by the cooling water within the control volume of Fig. 3.

$$\dot{Q} = \dot{m}_{\mathrm{cw}}(h_{\mathrm{cw2}} - h_{\mathrm{cw1}}) = \dot{m}_{\mathrm{cw}} c_{p\mathrm{cw}}(T_{\mathrm{cw2}} - T_{\mathrm{cw1}}) \tag{20}$$

On the other hand,

$$\begin{aligned}&\dot{m}_{s2}(e_{s1} - e_{s2}) + \dot{m}_a(e_{a1} - e_{a2}) + \dot{m}_{\mathrm{cond}}(e_{s1} - e_{\mathrm{cond}}) \\ &\quad = \dot{m}_{s2}(h_{s1} - h_{s2}) - T_o\dot{m}_{s2}(s_{s1} - s_{s2}) + \dot{m}_a(h_{a1} - \mathrm{h}_{a2}) \\ &\quad - T_o\dot{m}_a(s_{a1} - s_{a2}) + \dot{m}_{\mathrm{cond}}(h_{s1} - h_{\mathrm{cond}}) \\ &\quad - T_o\dot{m}_{\mathrm{cond}}(s_{s1} - s_{\mathrm{cond}})\end{aligned}$$

After algebraic manipulations and considering the first and second laws for the control volume, respectively, as

$$\sum_{\mathrm{in}} \dot{m}\, h = \sum_{\mathrm{out}} \dot{m}\, h \tag{21}$$

$$\dot{S} = \sum_{\mathrm{out}} \dot{m}\, s - \sum_{\mathrm{in}} \dot{m}\, s \tag{22}$$

it can be shown that

$$\begin{aligned}&\dot{m}_{s2}(e_{s1} - e_{s2}) + \dot{m}_a(e_{a1} - e_{a2}) + \dot{m}_{\mathrm{cond}}(e_{s1} - e_{\mathrm{cond}}) \\ &\quad = \dot{Q} + T_o[\dot{S} - \dot{m}_{\mathrm{cw}}(s_{\mathrm{cw2}} - s_{\mathrm{cw1}})]\end{aligned} \tag{23}$$

where $\dot{S}$ represents the entropy generation rate within the control volume.

Assuming the cooling water as an incompressible flow, one may apply the following equation to express its entropy change [16]:

$$s_{\mathrm{cw2}} - s_{\mathrm{cw1}} = c_{p,\mathrm{cw}}\, \ell n\left(\frac{T_{\mathrm{cw2}}}{T_{\mathrm{cw1}}}\right) \tag{24}$$

Substituting Eqs. (19), (20), (23), and (24) into Eq. (17) and simplifying the result gives

$$\eta_{\mathrm{ex}} = \left\{1 + \frac{N_s}{[(\frac{T_{\mathrm{cw2}} - T_{\mathrm{cw1}}}{T_o}) - \ell n(\frac{T_{\mathrm{cw2}}}{T_{\mathrm{cw1}}})]}\right\}^{-1} \tag{25}$$

where N_s is the entropy generation number defined as

$$N_s = \frac{\dot{S}}{C_{\mathrm{cw}}} \tag{26}$$

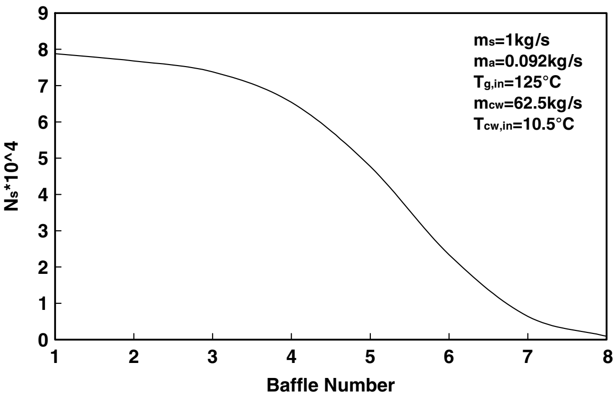

Fig. 14 Variation of the entropy generation number along the condensation path in a typical process condition.

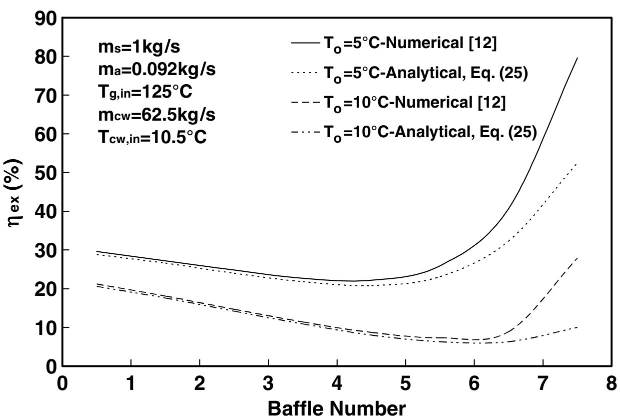

Fig. 15 Comparison of the exergy efficiency profiles resulting from the analytical expression in Eq. (25) and the numerical model [12].

Haseli et al. [11] studied the entropy production and related entropy generation number of condensation of steam in the presence of air. Thermal irreversibilities due to heat exchange between the bulk of the steam-air mixture and condensate, as well as heat transferred from the condensate and cooling water, were examined. It was shown that the latter term has a dominant role in the total entropy generation rate. Figure 14 shows a typical profile of the entropy generation number due to the thermal irreversibilities along the condenser. The exergy efficiency resulting from Eq. (25) at the same operating condition shown in Fig. 14 is also depicted and compared with the predicted results of the model presented in previous work [12] in Fig. 15 for two environment temperatures. Except for the last few baffle spaces, close agreement is achieved between the analytical [Eq. (25)] and numerical model [12]. The numerical model significantly overpredicts the exergy efficiency in the last few baffle spaces, in which the condensation of steam is almost finalized [10]. The resulting graphs depicted in Fig. 15 indicate that, as long as condensation of steam proceeds, the outcomes of Eq. (25) and the numerical model are compatible.

V. Conclusions

The local effectiveness of a horizontal shell and one-path tube exchanger that condenses steam from a mixture of air on the shell side with cooling water flowing inside the tubes is investigated based on a new definition of the maximum heat transfer rate. The effects of several process parameters are examined. In general, the local effectiveness increases along the condenser as condensation proceeds. After approximately finalizing the condensation process, however, it tends to decrease. Based on the numerical results, an empirical correlation is developed that relates the local effectiveness to the parameter c/θ. It enables us to observe their relation at a given inlet cooling water temperature and air mass flow rate. Moreover, an explicit equation is derived for evaluating the exergy efficiency of the system based on the entropy generation number, cooling water, and environment temperatures. The outcome of this analytical expression shows excellent agreement with the results of a numerical model.

Acknowledgment

The authors acknowledge the support provided by the Natural Sciences and Engineering Research Council of Canada.

References

[1] Browne, M. W., and Bansal, P. K., "An Overview of Condensation Heat Transfer on Horizontal Tube Bundles," *Applied Thermal Engineering*, Vol. 19, No. 6, 1999, pp. 565–594. doi:10.1016/S1359-4311(98)00055-6

[2] Semenov, V. P., Shklover, G. G., Usachev, A. M., and Semenova, T. P., "Enhancement of Heat Transfer in Condensation of Steam on a Horizontal Noncircular Pipe," *Heat Transfer: Soviet Research*, Vol. 22, No. 1, 1990, pp. 15–20.

[3] Xie, T., and Eckels, S. J., "An Investigation of Condensation Heat Transfer Performance of HFC-134a on Single Enhanced Tubes (RP-984)," *HVAC & R Research*, Vol. 9, No. 1, 2003, pp. 3–18.

[4] Briggs, A., "Enhanced Condensation Heat-Transfer on Mini or Low Fin Tubes," *Proceedings of the 4th International Conference on Nanochannels, Microchannels and Minichannels*, American Society of Mechanical Engineers, New York, 2006, pp. 1245–1253.

[5] Lienhard, J. H., IV, and Lienhard, J. H., V, *A Heat Transfer Text Book*, 3rd ed., Phlogiston Press, Cambridge, MA, 2006, Chap. 11.

[6] Incropera, F. P., *Introduction to Heat Transfer*, 5th ed., Wiley, Hoboken, NJ, 2007.

[7] Berg, W. F., and Berg, J. L., "Flow Patterns for Isothermal Condensation in One Pass Air Cooled Heat Exchangers," American Society of Mechanical Engineers Paper 79-WA/HT-5, 1979.

[8] Kayansayan, N., "Thermal Design Method of Bayonet-Tube Evaporators and Condensers," *International Journal of Refrigeration*, Vol. 19, No. 3, 1996, pp. 197–207. doi:10.1016/0140-7007(95)00079-8

[9] Wright, A. D., and Heggs, P. J., "Simplified Methodology for Calculating the Effectiveness of a Two Stream Plate Heat Exchanger with One Stream Undergoing a Phase Change," *Chemical Engineering Research and Design*, Vol. 80, No. A3, 2002, pp. 313–19.

[10] Haseli, Y., and Roudaki, S. J. M., "Simultaneous Modeling of Heat and Mass Transfer of Steam-Air Mixture on a Shell and Tube Condenser Based on Film Theory," *Proceedings of the ASME Summer Heat Transfer Conference*, Vol. 2, American Society of Mechanical Engineers, New York, 2003, pp. 251–259.

[11] Haseli, Y., Dincer, I., and Naterer, F. G., "Entropy Generation Number for Condensation of a Vapor in the Presence of a Non-Condensable Gas in a Shell and Tube Condenser," *International Journal of Heat and Mass Transfer*, 2007 (to be published).

[12] Haseli, Y., Dincer, I., and Naterer, F. G., "Exergy Analysis of Condensation of a Binary Mixture with One Non-Condensable Component in a Shell and Tube Condenser," *Journal of Heat Transfer*, 2007 (to be published).

[13] Haseli, Y., Dincer, I., and Naterer, F. G., "Optimum Temperature in a Shell and Tube Condenser with Respect to Exergy," *International Journal of Heat and Mass Transfer*, 2007 (to be published).

[14] Haseli, Y., Roudaki, S. J. M., "A Calculation Method for Analysis Condensation of a Pure Vapor in the Presence of a Non-Condensable Gas on a Shell and Tube Condenser," *Proceedings of the ASME Heat Transfer/Fluids Engineering Summer Conference*, Vol. 3, American Society of Mechanical Engineers, New York, 2004, pp. 155–163.

[15] Haseli, Y., "Study of Condensation of Steam in the Presence of Air on a Semi-Industrial Condenser Through a Proposed Algorithm," *Proceedings of the 2nd International Exergy, Energy and Environment Symposium*, Aristotle Univ. of Thessaloniki, Thessaloniki, Greece, 2005;also IEEES-05-52

[16] Moran, M. J., and Shapiro, H. N., *Fundamental of Engineering Thermodynamics*, 5th ed., Wiley, Hoboken, N. J., 2004.